Solvation shell effects and spectral diffusion: Photon echo and optical hole burning experiments on ionic dyes in ethanol glass

Dee William Pack,[a] L. R. Narasimhan, and M. D. Fayer
Department of Chemistry, Stanford University, Stanford, California 94305

(Received 23 October 1989; accepted 22 December 1989)

Results of picosecond photon echo and optical hole burning experiments are reported for four ionic dyes in ethanol glass. At low temperatures, the dephasing times deduced from the hole widths are as much as nine times shorter than those measured by the two-pulse echo because of the effect of spectral diffusion. The temperature dependences found are of the form $aT^{\alpha} + b \exp(-\Delta E/kT)$ due to glass two level system dynamics ($T < 4$ K) and a process that activates exponentially at higher temperatures, possibly from a pseudolocal mode or glass optical phonon. Comparing the ratios of echo to hole burning measured dephasing times for the four dyes suggests that the dephasing is influenced by the existence of distinct local ethanol solvation shells in addition to the dynamics of the bulk solvent. A theoretical description of solvent shell effects is achieved through the use of a two spatial domain model of the glass dynamics. Calculations of dynamic perturbations from distinct solvation shell and bulk solvent regions show that the observed differences between the dyes' dephasing ratios can be explained if the ionic chromophores alter glass dynamics locally.

I. INTRODUCTION

In the last several decades, considerable progress has been made in the development and application of line narrowing experiments in molecular spectroscopy. These techniques have allowed researchers to uncover subtle spectroscopic and dynamic effects from featureless, inhomogeneously broadened spectra and have found wide applications in many types of physical systems. As chromophores in increasingly complex host materials have been studied, an improved understanding of these experiments and what they measure has emerged.

Different types optical dephasing experiments have often been thought to measure the same dynamic parameter, the dephasing time T_2'. T_2' is a measure of the extent to which the environmental fluctuations perturb the energies of the ground and excited states of the optical transition in a probe molecule. Recent experimental[1-13] and comprehensive theoretical results[14-19] have shown that in systems such as glasses,[20,21] polymers,[20] and spin-active crystals,[7,17] the characteristic time scale associated with a particular experiment influences the result of the measurement. This is because complex systems possess a wide distribution of relaxation rates and various experiments are sensitive to different parts of the distribution. The dynamic decay times measured by various line narrowing techniques (such as two-pulse photon echoes,[2,3,11] stimulated photo echoes,[2,17] accumulated photon echoes,[2,10,11,14] incoherent accumulated echoes,[15] fluorescence line narrowing,[2] and persistent spectral hole burning,[2,3,8,9]) may differ significantly. A more complete understanding of low temperature dynamics in complex systems is possible when this is taken advantage of and techniques sensitive to a wide range of time scales are employed.[17]

In this paper, data from the line narrowing experiments with the fastest and slowest characteristic time scales, the two-pulse photon echo and persistent spectral hole burning are presented for four different ionic dyes in ethanol glass. The results discussed include the dramatic difference in the dynamic times measured by the two experiments, the temperature dependences of the optical dephasing rates, which are the signature of the active thermal processes, and possible evidence for a solvation shell effect in which the dye molecules themselves influence the dynamics. A two-domain theory for the effect of solvation on optical dephasing is developed and it can provide an explanation for these observations.

The data show that the low temperature values for the dephasing times from hole burning and photon echo experiments differ by factors between six and nine ($T_{HB}' \leqslant 6T_{PE}' - 9T_{PE}'$) for the four dyes in ethanol glasses. The explanation of this difference lies in the characteristic time span of the two techniques, typically hundreds of picoseconds for the two-pulse photon echo and hundreds of seconds for hole burning. In complex systems, such as glasses, dynamics can occur over a wide range of time scales from femtoseconds to hours and longer. The echo is sensitive to the fast fluctuations. Slower perturbations are rephased and eliminated. It measures what is generally referred to as the homogeneous dephasing time[2] $T_{PE} = T_2$. The hole burning experiment, which typically operates on a time scale of 12 or 13 orders of magnitude longer than the echo, is sensitive to slow rates in complex systems as well as faster processes. Slow relaxations which are rephased by a two-pulse echo are often referred to as spectral diffusion. The hole burning dephasing time is the combination of the homogeneous dephasing time and the additional contribution resulting from spectral diffusion (SD): $1/T_{HB} = 1/T_2 + 1/T_{SD}$. At low temperatures in ethanol glass, the dominant contributions to hole burning linewidths is from spectral diffusion. Through the complementary use of different techniques such as the photon echo and hole burning,[2,3,17] insights into the nature of fast and

[a] Permanent address: Infrared Sciences Department, Chemistry and Physics Laboratory, The Aerospace Corp., Los Angeles, CA 90009.

 0021-9606/90/074125-14$03.00 © 1990 American Institute of Physics

slow dynamics in glasses and other materials can be gained.

Recent work has shown that a four point correlation function is the proper description for a variety of line narrowing techniques. In particular, hole burning line profiles are the Fourier transform of the four point correlation function which describes the stimulated echo experiment.[2,17] This approach can properly describe the dependence of experimental observables on the finite time associated with an experiment. Hole burning is the frequency domain equivalent of the stimulated echo experiment and is, therefore, sensitive to spectral diffusion.

The temperature dependence of the two dephasing times T'_{HB} and T'_{PE} (the prime denotes the removal of the T_1 lifetime contribution) have been determined for several ionic dyes/glass systems. In general, at low temperatures ($T<4$ K), a power law temperature dependence is found: $1/T'_{EXP} = aT^{\alpha}$, where a is a constant and α is in the range 1.1–1.7. This holds for both the echo and hole burning dephasing times, as well as the spectral diffusion contribution T_{SD}. Power law dependences have been successfully derived using models for the distribution of two-level-system (TLS) well asymmetries and tunneling parameters of the glass.[20,22] The echo data show that fast relaxing two-level systems behave similarly to the slower ones probed by hole burning. At higher temperatures in these dye/glass systems ($T<4$ K), an exponential term $b\exp(-\Delta E/kT)$ dominates the dephasing.[1-3]

Taking the ratio T'_{PE}/T'_{HB} permits an interesting comparison of different dyes in the same host glass.[2,3,16] The ratio divides out the strength of the coupling of the dyes to the environment and reflects only the TLS dynamics. The ratio is determined by the distribution of tunneling rates in the glass. The larger the ratio, the more dynamic perturbations of the probe molecule take place in the time span between the two experiments. The ratio, and by implication, the distribution of rates might be expected to be a unique property of the bulk glass. However, in the experiments on the ionic dyes in ethanol glass presented below, this is shown not to be the case. The dye molecules alter the distribution of relaxation rates which they sample and do so in different ways. It is proposed that this is due to structural differences of the solvation shells of different ionic dye molecules. The probe chromophores employed are resorufin, cresyl violet, sulforhodamine 640, and rhodamine 640. These ionic dyes differ in structure and also in their charge distribution, e.g., resorufin is a -1 anion, cresyl violet is a $+1$ cation. The largest change in the ratio is observed when going from the positive ion to the negative ion. The change in charge will have a major influence of the solvent shell structure and, therefore, the dynamics.

II. EXPERIMENTAL PROCEDURES

The four ionic dyes used as optical probes in this study are cresyl violet 670 perchlorate (CV); rhodamine 640 perchlorate (R640); sulforhodamine 640 (S-R640), a zwitterion; and resorufin (Res), a Na^+ salt. These were purchased from Exciton and Aldrich and used without further purification. Samples of approximately 2×10^{-4} M were prepared in three isotopically distinct ethanol solvents C_2H_5OH (Rossville gold shield), C_2H_5OD, and C_2D_5OD (Aldrich). The deuterated solutions were prepared in an argon atmosphere after degassing the ethanol with argon.

Ethanol can form three phases depending on the sample's thermal history, an amorphous phase (phase I), a plastic crystalline phase (phase II), and a crystalline phase.[23,24] Rapid cooling to liquid He temperature insures the preparation of the amorphous phase.[23] Samples were transferred to a 1.0 mm optical glass cuvette and fast quenched (>100 K/min) in liquid He. All echo and hole burning data were taken on identically cooled samples of ionic dyes in the glassy phase of ethanol (phase I). Experiments were done at temperatures between 1.0 and 13.0 K. Two cryostats were used, an immersion dewar for $T=1.0$–2.1 K, and a temperature regulated Janis immersion and flow dewar for 1.4–13.0 K measurements. Temperature was measured with a calibrated germanium resistance thermometer in excellent thermal contact with the sample[5] and was regulated to ±0.05 K.

The laser systems used to perform these experiments have been described previously in detail.[1] The photon echo is performed with an amplified, synchronously pumped dye laser which produces tunable 1.5 μJ, 4 ps pulses with an 11 cm^{-1} bandwidth at 0.7 kHz repetition rate. A pulse is beam split and attenuated so each pulse is approximately 70 nJ. This eliminates possible optical density effects.[25] Echo decays at a range of power levels were taken to insure the results presented are independent of power,[25] and that no unwanted heating occurs. The two pulses are focused at a 1°-degree angle in to a clear spot in the glass sample. This is aided by a colinear, low power HeNe beam which is used to find clear regions in the cracked vitreous ethanol. The echo comes off at an angle determined by phase matching and is spatially separated by an iris before detection by a photodiode. Motorized delay lines allow the pulse separation to be scanned to measure the echo decay. One beam is chopped at half the laser repetition rate and the signal is fed to a lock-in amplifier and a x–y recorder. Decays are then digitized and analyzed on a PC. The laser is tuned to the red side of the inhomogeneous bands of the four dyes. This avoids the unwanted excitation of vibronic transitions. Hole burning and photon echo measurements were performed at the same frequencies in the various dyes. Echo experiments performed at different frequencies within a few nm of the chosen wavelengths on the red side of the absorption band exhibit identical decays. This insures that no significant site-dependent dynamics occurs over the bandwidth of the laser pulses. An ensemble of molecules with the same dynamics are probed by both experiments. The bulk of the experimental measurements were taken at the following wavelengths: resorufin—584 nm; cresyl-violet—616 nm; rhodamine 640—590 nm; sulforhodamine 640—596 nm.

The hole burning that occurs during a PE measurement is corrected following the method of Berg *et al.*[2] This involves recording the echo intensity with a fixed pulse separation as a function of time. As the sample undergoes hole burning the echo signal is reduced, typically by about 30%–40% in C_2H_5OD samples during a standard 4 min recording period. These "burning curves" are then used to normalize

the echo decay curves, eliminating the effect of hole burning from the echo decays. Such a procedure requires the laser be focused to a new, unburned spot for every echo decay and burning curve. C_2H_5OH samples burn about 60 times faster. (The hole burning mechanism has been demonstrated to be due to a double hydrogen bond rearrangement for resorufin/ethanol.)[26,27] To avoid such rapid burning, echo studies reported here were confined to deuterated ethanol. Echo results were previously shown to be independent of deuteration for resorufin/ethanol glass.[1,2]

Holes are burned and read in transmission with a frequency stabilized dye laser (Coherent CR-599-21, 1.5 MHz jitter). This laser was altered so the thin etalon could be computer controlled, extending the scanning range from 30 to 90 GHz. This is useful for measuring full line profiles of the broader, high temperature holes. The beam is split just before the dewar and laser power is monitored by a photodiode for a reference. The signal is detected with a cooled photomultiplier tube. For some experiments the laser was chopped at 400 Hz and lock-in detection was used. In more recent experiments, the photomultiplier tube, (PMT) and photodiode (PD) outputs were fed directly into a ratiometer and the output voltage sent to a PC. Laser power is altered between burning and reading power levels with tandem acousto-optic modulators. This precisely maintains beam direction and allows computer control of the laser power setting. Laser fluence levels were set so hole depths of 0.5%–2% were produced. Hole widths were independent of fluence for such shallow holes. Typical low temperature values were 1 μ W/cm^2, 3 s exposure for C_2H_5OH and 10 μW/cm^2, 5 s exposure for C_2H_5OD. Higher temperatures required higher fluences typically of 120 and 1200 μJ/cm^2, respectively, for C_2H_5OH and C_2H_5OD, and were achieved with the same power levels, but longer exposure times. Reading power levels were typically 100 times less, to insure that no significant burning occurred while a hole was being read. Computer or manually controlled shutters were used to isolate detectors from burning power levels and to expose the sample for a precise irradiation time.

Since the hole linewidth is sensitive to spectral diffusion, which widens the hole, the characteristic time scale of the experiment, T_W, is important.[2,17] Essentially, T_W is the time from burning through reading a hole.[17] For most of the holes measured in this study, T_W was kept in the range 200–600 s. Detailed time-dependent hole burning experiments on cresyl violet and resorufin have shown that very little hole broadening occurs over this limited time span in ethanol, so the time dependence of the spectral diffusion introduces no significant error in comparing hole widths.[4,5] (Note that over a broader range of times the hole width increases significantly[4,5] and the time behavior will differ for different hosts.[5]) Accurately knowing and controlling T_W is important when analyzing hole burning results and comparing results between different laboratories.

Fluorescence lifetimes were measured for the dye solutions studied to remove the T_1 contribution from the dephasing time. Two apparatuses were used. The first excited emission with 70 ps pulses from a mode-locked, q-switched Nd:YAG laser and monitored the fluorescence decay with a microchannel plate and a transient digitizer (instrument response time 1.0 ns). The second was a time-correlated single photon counting setup. This used a mode-locked, cavity dumped dye laser (10 ps pulses) pumped by a mode-lock Nd:YAG laser to excite emission and monitored the transient with a photomultiplier tube (instrument response time 1.1 ns). The optical density of samples was kept below 0.1 to avoid reabsorption of emission and dilutions verified that the lifetimes were independent of concentration. The lifetimes are shown in Table I along with a specific list of experiments performed on the various dye/glass systems. The photon echo and hole burning results of Walsh *et al.*[1] and Berg *et al.*[2] on Res/C_2H_5OH and Res/C_2H_5OD are included in the following discussions. New data collected on these systems agreed with their previous results.

TABLE I. Experiments performed on dyes in three types of deuterated ethanol. Two-pulse photon echo is abbreviated PE. Spectral hole burning is abbreviated HB. Fluorescence lifetimes T_1 are also listed.

Dye solution		Experiments PE	Experiments HB	T_1 (ns)
Resorufin	C_2H_5OH	X	X	3.9
	C_2H_5OD	X	X	4.2
Cresyl violet	C_2H_5OH		X	3.3
	C_2H_5OD	X	X	5.5
	C_2D_5OD		X	
Sulforhodamine 640	C_2H_5OD	X	X	4.6
Rhodamine 640	C_2H_5OD	X	X	4.4

III. THEORY OF HOLE BURNING AND PHOTON ECHOES IN GLASSY SYSTEMS

A series of recent papers have presented the theoretical description of optical dephasing experiments in glasses, including hole burning and photon echoes,[2,14–19] The four point correlation function formalism is used, which predicts that the results of the experiment will depend on a time T_W, the characteristic time scale of the experiment.[2,14–17] The photon echo's correlation function[2,17] has the shortest experimental scale ($T_W = 0$) and measures the longest dephasing time (narrowest linewidth). The T_2 the echo measures is generally referred to as the homogeneous dephasing time.[2]

The theory is recapitulated as necessary so that it can be extended to study situations with nonuniform spatial distributions of tunneling TLS. A simple two-domain model is proposed to account for solvation shell phenomena. This allows calculations to be made for physical systems such as strongly solvated dyes in glasses and chromophores in porous media or inside micelles in a glass host. Related calculations for adsorbed molecules on surfaces, with two-dimensional distributions of TLS, have recently been presented.[28]

A. Hole burning

The spectral profile of the hole, neglecting T_1 (lifetime) contributions, is proportional to the Fourier transform of

the four point, or stimulated echo correlation function $C(\tau,T_W,\tau)$[17]:

$$I_H(\omega) = \int_{-\infty}^{+\infty} d\tau \exp(i\omega\tau) C(\tau,T_W,\tau), \quad (1)$$

where $C(\tau,T_W,\tau)$ is

$$C(\tau,T_W,\tau) = \left\langle \exp\left[i \sum_j^N \phi_j(\tau,T_W) \right] \right\rangle, \quad (2)$$

N is the number of perturbing TLS in the averaging volume, and $\langle\cdots\rangle$ represents the averages over the stochastic history, spatial distribution, and internal parameters of the TLS. $\phi_j(\tau,T_W)$ is the phase perturbation caused by the tunneling TLS. Adopting the sudden jump model for the time variation of the chromophore's optical frequency, $\phi_j(\tau,T_W)$ is the function[29,30]

$$\phi_j(\tau,T_W) = \Delta\omega_j \left[\int_0^{\tau} h(t)dt - \int_{T_W+\tau}^{T_W+2\tau} h(t)\,dt \right], \quad (3)$$

where $\Delta\omega_j$ is the perturbation of the chromphore's optical frequency by the jth TLS. $h(t)$ is a random telegraph function that takes on the values $+1$ or -1 depending on the state of the TLS. The time limits in the integrals of Eq. (3) are straightforward for a stimulated echo. τ and T_W are defined as the delays between the first and second pulses, and the second and third pulses, respectively. The stimulated echo is generated at time $T_W + 2\tau$ later. For the hole burning experiment, τ is the lifetime of the coherent polarization induced during the burning and reading pulses, essentially the T_2 that a two-pulse echo would measure.[2,17] T_W is basically the time required to perform the experiment from burning through reading the hole.[2,17] In hole burning, T_W is typically many orders of magnitude longer than τ, minutes as compared to nanoseconds.

The correlation function is set up in Eq. (2) as an average of the perturbation of N TLS on the frequency of a single reference chromophore. This is valid for a low concentration sample. The sum Σ_j corresponds to a particular configuration of N TLS around a chromophore. If the perturbers are assumed to be noninteracting and statistically independent, the exponential in Eq. (2) can be factored into a product of N identical terms and simplified to give[29,32]

$$C(\tau,T_W,\tau) = \langle \exp[i\phi(\tau,T_W)] \rangle^N. \quad (4)$$

Using

$$\lim_{N\to\infty} \left(1 - \frac{y}{N}\right)^N = \exp(-y),$$

Eq. (4) becomes

$$C(\tau,T_W,\tau) = \exp\{ -N \langle 1 - \exp[i\phi(\tau,T_W)] \rangle_{H,r,E,R} \}. \quad (5)$$

The averages are over the stochastic history path H, the spatial distribution r, and the microscopic parameters of the TLS, the splitting energy E and the relaxation rate R. The relaxation rate to equilibrium is the sum of the up, down TLS transition rates.[14] For one phonon processes, $R \propto e^{-\lambda E} \coth(E/2kT)$. (The tunneling parameter $\lambda = d(2MV/\hbar)^{1/2}$ is the wave function overlap and depends on tunneling distance d, mass M, and barrier height V.[33])

The history average may now be performed. Using the result of Bai and Fayer[17] for the long-time limit $T_W > 10\tau$, the hole burning correlation function is

$$C(\tau,T_W,\tau) = \exp\{ -N \langle \sin^2(\Delta\omega\tau)\mathrm{sech}^2(E/2kT) \times [1 - \exp(-RT_W)] \rangle_{r,E,R} \}. \quad (6)$$

These manipulations follow the spin resonance results of Refs. 29–32. Performing the history average first,[17] however, has been shown to aid in the evaluation of nonuniform distributions of perturbers and keeps the treatment more general. Also, the imaginary term in the calculation cancels naturally in the history average[17] avoiding the need to introduce approximations eliminating it.[31,32,34]

For the case in which the chromophore has little effect on the TLS dynamics, the spatial average may be separated from the averages over E and R [17]:

$$\langle \sin^2[\Delta\omega(r)\tau] \rangle_r \times \langle \mathrm{sech}^2(E/2kT)[1 - \exp(-RT_W)] \rangle_{E,R}. \quad (7)$$

The spatial average $\langle\cdots\rangle_r$ determines the shape of the correlation function decay and, therefore, the line profile. It will vary depending on the form chosen for the perturbation $\Delta\omega$ and the spatial distribution of TLS. The average over E and R, $\langle\cdots\rangle_{E,R}$, contributes a temperature and time-dependent weighting factor for the number of TLS that have tunneled and perturbed the reference chromophore under the given experimental conditions. This makes the correlation function decay and linewidth a function of temperature and time, the form of which is determined by the distribution of E and R.

The spatial average is now evaluated for a dipolar interaction between the chromophores and TLS, and initially for a random spatial distribution of perturbers $P(r) = dV/V$. These choices have been shown[2,29–32] to lead to exponential correlation function decays and Lorentzian line shapes consistent with experimental results.[22] The TLS dipoles involved could be either electric or elastic strain dipoles. The frequency perturbation is then

$$\Delta\omega(r,\Omega) = D\kappa(\Omega)/r^3, \quad (8)$$

where r is the distance between a TLS and a chromophore, and $\kappa(\Omega)$ is the orientational factor for dipolar coupling. D is the dipolar coupling constant $D = \Delta\mu_M \Delta\mu_{\mathrm{TLS}}$. The magnitude of the change in dipole moment $\Delta\mu$ between the two states of the optical center and the tunneling states determines the coupling strength. The dipolar orientational average $\langle|\kappa(\Omega)|\rangle_\Omega$ is a term on the order of one.[35] It can be explicitly calculated for electric dipole interactions. For elastic dipole interactions $\langle|\kappa(\Omega)|\rangle_\Omega$ is a function involving the strain tensors of the medium. An approximate calculation in this case gave the value 0.87.[36] In what follows, this term is included in D and should be considered $D(\Omega)$. The spatial average calculation has been done before.[29–32,35,37,38] To model solvation shell effects later, we must consider an altered form of it for nonisotropic distributions of perturbers.

The spatial average is

$$\langle \sin^2(\Delta\omega\tau)\rangle_r = \int_0^{2\pi} d\phi \int_0^{\pi} \sin\theta\, d\theta \int_0^{\infty} r^2\, dr \sin^2\left(\frac{D}{r^3}\tau\right) \tag{9}$$

$$= \frac{4\pi}{3}\int_0^{\infty} dx \frac{\sin^2(D\tau x)}{x^2} \tag{9a}$$

$$= \frac{2\pi^2}{3} D\tau. \tag{9b}$$

The variable change $x = 1/r^3$ is used to simplify Eq. (9). The correlation function is then

$$C(\tau,T_W,\tau) = \exp\left[-\frac{2\pi^2}{3} n(T,T_W) D\tau\right]. \tag{10}$$

In writing Eq. (10), the density of TLS, $n = N/V$, is multiplied by the average over E and R, $\langle\cdots\rangle_{E,R}$, to give the *density of active TLS* that cause dephasing at the optical centers $n(T,T_W)$. The hole correlation function decays exponentiallly and the hole profile [Eq. (1)] is Lorentzian. The contribution of population decay T_1 processes is not included in Eq. (10),[2,17] so comparisons should be made to lifetime corrected data. Results in a similar form were obtained by Black and Halperin[36] and Reineke[39] for phonon echoes and fluorescence line narrowing experiments, respectively. These studies did not explicitly consider the experimental time scale T_W. Combining all of the factors in Eq. (10) into a decay rate $\Gamma_{HB} = (2\pi^2/3)n(T,T_W)D$, the Fourier transform will give a Lorentzian with full width at half-maximum (FWHM) $= \Gamma_{HB}/\pi$. This is the actual width of the hole (minus the lifetime contribution). The two interactions with the radiation field during burning and reading are built in to the four point correlation description. As discussed previously by Berg *et al.*,[2] the factor of 2 necessary to extract the hole burning measured dephasing time T'_{HB} (no lifetime contribution) arises from the consistent definition of the decay of the macroscopic polarization as[2]

$$P_{HB} \propto \exp(-2\tau/T'_{HB}). \tag{11}$$

So, $1/T'_{HB} = \Gamma_{HB}/2$ and in terms of the experimentally measured linewidth $1/T'_{HB} = \pi(\text{FWHM}/2) - 1(2T_1)$, where removal of the lifetime contribution has been included. It is this consistently defined dephasing time that is compared to the results of other experiments such as photon echoes.

The thermally active concentration of TLS, $n(T,T_W)$, reflects the underlying glass distribution of tunneling energies E and relaxation rates R.

$$n(T,T_W) \propto \langle \text{sech}^2(E/2kT)[1-\exp(RT_W)]\rangle_{E,R} \tag{12}$$

or

$$n(T,T_W) \propto \int dR\, P(R)[1-\exp(RT_W)], \tag{13}$$

where $P(R)$ is defined as the average of thermally accessible TLS relaxation rates[4,5,17]

$$P(R) \propto \int dE\, P(E,R)\,\text{sech}^2(E/2kT). \tag{14}$$

In a common model for low temperature glass dynamics, the TLS energies E and tunneling parameter λ are assumed to be uniformly distributed, at least over the ranges active at low temperature, i.e., $P(E) = P_E$; $P(\lambda) = P_\lambda$. Such distribution of TLS parameters were used to obtain a linear term in the low temperature specific heat of glasses.[40,41] The observation of a term close to linear[42] first attracted extensive theoretical interest in glass dynamics. When combined with the definition of R,[14] these uniform functions lead to a distribution of relaxation rates proportional to $1/R$, $P(R) = P_R/R$.[43] Integrating over these distributions in Eq. (12) leads to $n(T,T_W)$ and the hole width, increasing linearly with temperature and logarithmically with increasing waiting time T_W between burning and reading a hole.[14] A slowly increasing energy distribution function of the form $P(E) = P_E E^\mu$ $(0<\mu<1)$ leads to a linewidth proportional to $T^{1+\mu}$.[20,22] Such a temperature dependence has been observed in this study and many others.[20] A firm physical model for nearly constant TLS distribution functions, or for other choices,[44] is lacking. Later when comparing results from different dyes in ethanol glass to theoretical results dependent on $n(T,T_W)$, data taken at the same temperature and experimental waiting times T_W are used, so the exact choices of TLS distribution functions do not affect the conclusions.

B. Two-pulse photon echo

The photon echo correlation function is now presented. Following a series of steps analogous to Eqs. (2)–(5), the photon echo decay function $C(\tau,0,\tau)$ is written:

$$C(\tau,0,\tau) = \exp\{-N\langle 1-\exp[i\phi(\tau,0,\tau)]\rangle_{H,r,E,R}\}, \tag{15}$$

where $\phi(\tau,0,\tau)$ is

$$\phi(\tau,0,\tau) = \Delta\omega\left[\int_0^{\tau} h(t)dt - \int_{\tau}^{2\tau} h(t)dt\right]. \tag{16}$$

This function has been evaluated[22,45,46] with the same model used above: sudden jump perturbation by tunneling centers, dipolar interaction, a random distribution of perturbers, and the commonly used glass distribution functions $P(E) = P_E E$ and $P(R) = P_R/R$. Following Refs. 45 and 46, the ensemble averages are performed yielding the exponential decay function

$$C(\tau,0,\tau) = \exp\left(-\frac{2\pi^2}{3} n(T) D\theta\tau\right). \tag{17}$$

$n(T)\theta = N/V\langle\cdots\rangle_{E,R}$, where $n(T)$ is the temperature-dependent concentration of active TLS. $n(T)$ is different from $n(T,T_W)$ [see Eqs. (12) and (13)] in that it is the concentration of active TLS with fast rates (echo time scale), while $n(T,T_W)$ is for fast and slow rates out to the T_W time scale, θ is a number resulting from the evaluation of the integrals over H, E, and R and is found by Maynard *et al.* to be *3.66*.[45,46] (Obtaining this value requires the results of an important erratum[46] and an account of a factor of 2 in the change of variables associated with the splitting energy E. Note in a previous paper[3] the error of Ref. 45. Numerical integration of the equations from Refs. 45 have verified 3.66 as the correct number.) For a constant energy density of

states $P(E) = P_E$, $n(T) \propto T$. Distributions of the form $P(E) \propto E^{\mu}$ yield $n(T) \propto T^{\mu}$.[22] The photon echo correlation function decay rate is $\Gamma_{PE} = (2\pi^2/3)n(T)D\theta$. T_1 processes have been omitted from Eq. (17). The relationship between the correlation function decay and experimental observables may be made clear by first noting that the decay of the macroscopic polarization for the photon echo is (with no lifetime contribution)

$$P_{PE} \propto \exp(-2\tau/T_2'), \tag{18}$$

$T_2' = T_{PE}'$. Removing the emission lifetime T_1 contribution is accomplished using $1/T_{PE}' = 1/T_{PE} - 1/(2T_1)$ and $1/T_{PE}' = \Gamma_{PE}/2$. The experimental photon echo signal is proportional to the square of the macroscopic polarization, so the raw data decays as $\exp(-4\tau/T_2)$.[47,48]

C. Comparing the photon echo and hole burning measurements

The ratio of the dephasing times measured by photon echo and hole burning experiments, at a given temperature, provides insight into the amount of perturbation of the chromophore by slow dynamical processes. Taking the ratio divides out the effect of chromophore–glass coupling parameters and give a measure of the amount of spectral diffusion in a given system. To calculate the ratio $R_d = T_{PE}'/T_{HB}'$, we note that the hole burning correlation function may always be split into parts corresponding to the fast dynamics measured by the echo and the spectral diffusion contribution $C(\tau,T_W,\tau) = C(\tau,0,\tau)\ C(\tau,T_W,\tau)$.[2,16] The ratio is then

$$R_d = \frac{T_{PE}'}{T_H'} = 1 + (1/\theta)\langle 1 - \exp(-RT_W)\rangle_R. \tag{19}$$

In Eq. (19), the spectral diffusion calculation $C(\tau,T_W,\tau)$ introduces a term

$$\langle 1 - \exp(-RT_W)\rangle_R = \int_{R_{min}}^{R_{max}} dR\, P(R)\,[1 - \exp(-RT_W)]. \tag{20}$$

To a good approximation, $R_{max} = \Gamma_{PE} = 2/T_{PE}$, and $R_{min} = 1/T_W$[2,16] for a distribution of rates that extends out to or past the inverse of the experimental time scale. Here, it is made clear that the spectral diffusion contribution to T_{HB}' is due to the dynamics occurring on a time scale longer than the echo time scale out to the waiting time of the experiment T_W. Using the glass model $P(R) \propto 1/R$ in Eq. (20), Eq. (19) is evaluated to give[16]

$$R_d = \frac{T_{PE}'}{T_{HB}'} = \frac{1}{\theta}\left[\theta + \ln\left(\frac{2T_W}{T_2}\right)\right]. \tag{21}$$

If chromophores do not significantly influence glass dynamics, R_d should be the same for various dyes in the same glass. Assuming for the moment that the simple rate distribution $P(R) \propto 1/R$ holds, R_d can be calculated. For our experiments on ionic dyes in ethanol, $T_2 \approx 1$ ns, $T_W \approx 200$ s, and the dephasing ratio is calculated to be $R_d = 8.3$. In Eq. (20), integration over a $1/R$ distribution of rates predicts a logarithmic increase of hole width with the waiting time T_W. Such logarithmic increases in hole widths have been observed in doped glasses.[12,13] Recent time-dependent studies at time scales down to 0.1 s demonstrate that the rate distribution is more complex than a simple $1/R$ model.[45] Nonetheless, Eq. (21) is useful in discussing dyes in the same glass with different experimental dephasing ratios.

IV. THE TWO-DOMAIN MODEL FOR SOLVATION SHELL EFFECTS ON GLASS DYNAMICS

In this section, the correlation function approach outlined above is extended to study nonuniform distributions of perturbers; specifically, to investigate the effect on experimental observables of the alteration of local dynamic behavior by a chromophore. A simple two-domain model is a logical first step. We assume within a spherical shell of radius r_s the nature of the tunneling TLS may differ from the bulk glass. This is illustrated in Fig. 1. While such an approach can be employed to calculate changes in both echo decays and hole burning line shapes, the following discussion is restricted to the latter, since consideration of hole burning is sufficient to discuss the experimental results and allows one to take advantage of the simplicity of the average over rates in the long time limit.

The correlation function is now calculated in two parts: one for the inner solvation shell, and one for the bulk glass, each with its own distribution of TLS properties. Since the perturbers in both regions may be treated with the sudden jump model, the history average is unaltered. Equation (6) is divided into two parts:

$$C(\tau,T_W,\tau) = \exp[-N_1\langle Q_1(r,E,R)\rangle_{r,E,R} - N_2\langle Q_2(r,E,R)\rangle_{r,E,R}], \tag{22}$$

where the subscripts 1 and 2 refer to the solvation shell and outer regions, respectively. Using Eqs. (7)–(9), the two-domain correlation function is rewritten as the sum of the active TLS concentration times the spatial distribution inte-

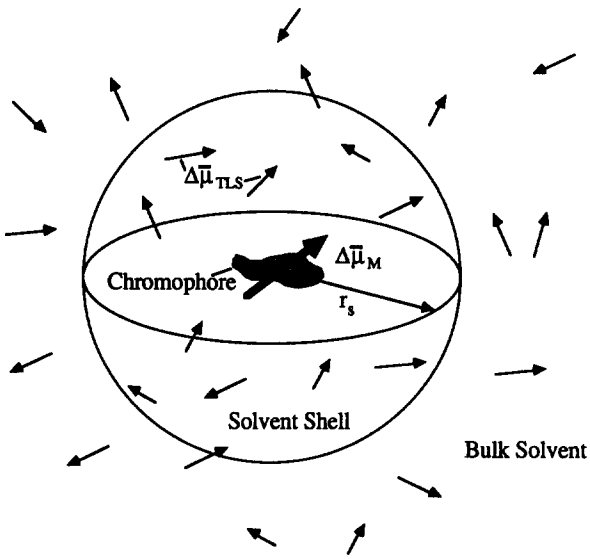

FIG. 1. A depiction of the two-domain model with solvation shell radius r_s. A chromophore with a ground to excited state dipole moment change $\Delta\mu_M$ is surrounded by a random distribution of TLS with dipolar changes $\Delta\mu_{TLS}$ associated with jumps between the two states. Glass dynamic properties may vary between the shell and bulk regions.

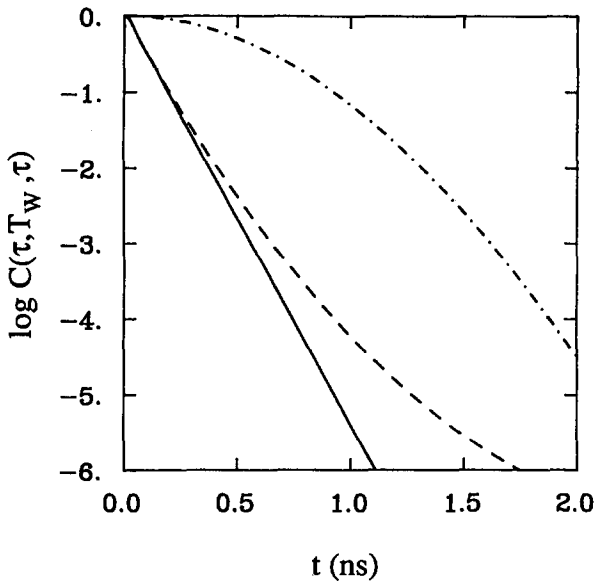

FIG. 2. Temporal behavior of the hole burning correlation function $C(\tau,T_W,\tau)$ divided into two regions: -·-·-, outside r_s; - - -, inside r_s; and —, the combined function. Parameters used are $r_s = 20$ Å, $n_1(T,T_W) = n_2(T,T_W) = 7\times10^{-4}$ TLS/Å^3, $D = 2.73\times10^{12}$ Hz Å^3.

grals:

$$C(\tau,T_W,\tau) = \frac{4\pi}{3}\left[n_1(T,T_W)\int_{1/r_s^3}^{\infty} dx\,\frac{\sin^2(D\tau x)}{x^2} + n_2(T,T_W)\int_0^{1/r_s^3} dx\,\frac{\sin^2(D\tau x)}{x^2}\right]. \quad (23)$$

When $n_1(T,T_W) = n_2(T,T_W)$, the isotropic case is recovered, with an exponentially decaying correlation function leading to a Lorentzian hole profile. Figure 2 illustrates the isotropic case for a particular set of $n(T,T_W)$, D and r_s values. Numerical solutions are plotted for the two halves of Eq. (23), inside and outside of the solvation shell. The combined function, which decays exponentially, is also plotted. The nearest perturbers are responsible for the short time decay of the correlation function and, therefore, the wings of the line shape. The more distant perturbing TLS contribute to the correlation function decay at longer time and influence the center part of the line shape. This has been noted before in calculations of echo decay functions.[18,19]

When $n_1(T,T_W) \neq n_2(T,T_W)$ due to a change in the local environment, a nonexponential correlation function decay and a non-Lorentzian line shape result. When the isotropic distribution of perturbers is altered and limits set on the integral in the spatial average, the function is no longer analytically solvable and a numerical integration must be performed. The two region devision of the glass surrounding the optical center is a simplified model for the interaction with the solvent. For instance, if the TLS rates were affected through an ion–dipole interaction $(1/r^2)$, $n(T,T_W)$ would be dependent on distance within the solvation shell. The concept of a shell cutoff is justified through the existence of a dipolar shielding term. In the absence of a detailed microscopic model for TLS dynamics, we feel that a two-domain approach is a useful first step in investigating the impact of chromophore–glass interaction on optical observables such as hole burning. While the integral equation approach of Eq. (23) is appropriate for a glassy host, for a crystalline system a better method is to start with Eq. (2) and take the sum over discrete lattice sites. This was the approach of Bai and Fayer in their model for spin–spin-induced dephasing of Pr^{+3}:CaF_2.[17] A hybrid approach, using a summation for *nearby* crystal sites and an integral calculation for distant ones, was adopted by Grant and Stranberg for the calculation of spin–spin interactions in crystals.[38]

We will consider the solvent shell and the bulk separately before recombining them. The two pieces provide simple models for other physical situations. For instance, the inner shell calculation could correspond to the behavior of an optical probe species inside a reverse micelle, or inside the solvent containing pores of a Vycor glass host. For such a model to apply, the dynamics of the TLS of the outer region must be unimportant in comparison to the core. Such a restriction might only strictly apply to chromophores trapped in tiny inclusions in crystals. The outer shell (bulk) calculation taken alone shows the effect of totally freezing nearby dynamics. This represents the ultimate limit of any solvation shell effect, rendering of the nearby species as "crystal-like", and eliminating the glassy degrees of freedom. Further numerical evaluation of Eq. (23), and Fourier transforming it to obtain model line shapes, is presented in Sec. VI, following a discussion of experimental data in the next section.

V. RESULTS AND DISCUSSION

A. The temperature dependence of the photon echo and hole burning

Figure 3 shows echo decays and holes measured on two of the four dyes studied in ethanol glass at 1.5 K. In all four dyes, echo decays are exponential and the hole profiles are well fit by Lorentzian line shapes over the entire temperature range investigated. For each of the dye/glass pairs, the dephasing times measured by the photon echo T'_{PE} are dramatically longer than those derived from the hole width T'_{HB} by factors of 6 to 9 [lifetime correction is made for T'_{PE} using $1/T'_{PE} = 1/T'_{PE} - 1/2T_1$, and for T'_{HB} using $T'_{HB} = (\pi\text{FWHM}/2 - 1/2T_1)^{-1}$]. This demonstrates that the hole widths are dominated by spectral diffusion, slow perturbations caused by glass TLS degrees of freedom, and do not measure what is normally thought of as a homogeneous linewidth. Instead, the dynamic time measured by the hole is due to the contribution of both the fast *and* slow processes $1/T'_{HB} = 1/T'_{PE} + 1/T_{SD}$. To emphasize the differences in echo and hole measured dephasing times, the holes are shown in Fig. 3 along with the corresponding line shapes obtained from the echo data.

Figure 4 plots the temperature dependences of T'_{PE} and T'_{HB} for resorufin[2,3,40,50] and cresyl violet[3,51] in ethanol glasses. For both dye/glass systems the echo and hole burning dephasing times are well fit by functions of the general form[1–3]

$$1/T'_{exp} = aT^{\alpha} + b\exp(-\Delta E/kT). \quad (24)$$

This type of composite temperature function, with a power law due to the low temperature glass TLS perturbations and

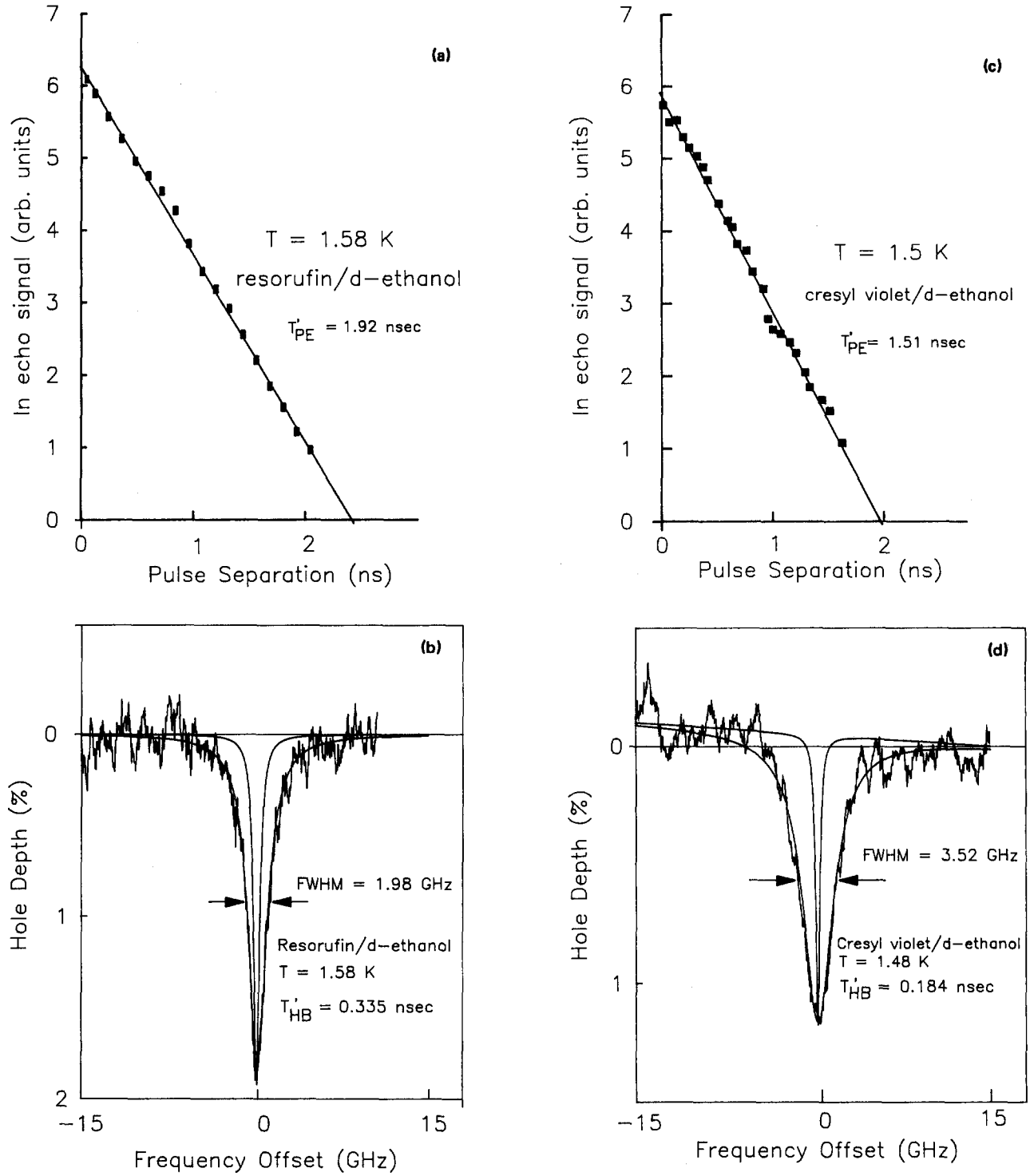

FIG. 3. A comparison of photon echo and hole burning data for two of the four ionic dyes in ethanol glass: (a) and (b) resorufin/CH_3CH_2OD, (c) and (d) cresyl violet/CH_3CH_2OD. The echo decay data are plotted with best fit lines yielding $T_2/4$. The hole widths are plotted with best-fit Lorentzians (solid lines). The comparable linewidths obtained from echo data are also plotted. The much narrower Lorentzians obtained from the echo data illustrated the extra broadening of the holes by spectral diffusion. Lifetime corrected dynamics times T'_{PE} and T'_{HB} differ by factors of 6–9.

an exponentially activated term, was first suggested by Jackson and Silbey.[52] The exponential term may be caused by activation of a pseudolocal mode of the dye, such as a libration, or to glass optical phonons which could be localized due to the disorder in the glass (essentially ethanol pseudolocal modes). An exponential term can also result from potential barrier crossing,[13] at least for a narrow distribution of barrier heights. Table II shows the results of several different fits for the photon echo and hole burning results. The procedure used is to first perform a least-squares fit of the low temperature data ($T < 3$–4 K) to aT^{α}. This term is then subtracted from the higher temperature data and the best fit

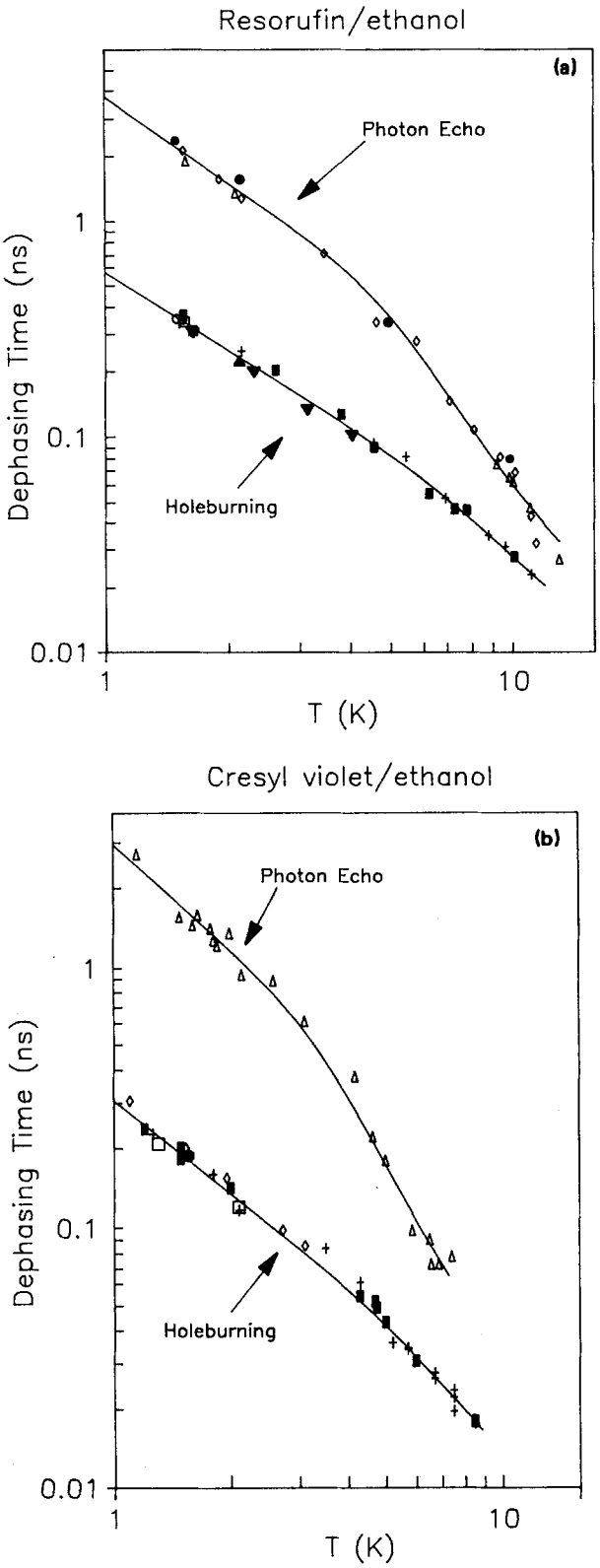

FIG. 4. Temperature dependences of photon echo (T'_{PE}) and hole burning (T'_{HB}) data with fits to model Eq. (24). (a) resorufin/ethanol: *photon echo*—CH_3CH_2OH host, ◇ [Berg *et al.* (Ref. 2)]; CH_3CH_2OH host, ● [Berg *et al.* (Ref. 2)] △ (Ref. 3 and this work); *hole burning*—CH_3CH_2OH host ■ [Berg *et al.* (Ref. 2)], ○ (Ref. 3 and this work), ▲ [Littau *et al.* (Refs. 4 and 5), ▼ [Van Den Berg and Völker (Ref. 49)]; CH_3CH_2OD host, + [Berg *et al.* (Ref. 2)], □ (Ref. 3 and this work). (b) Cresyl-violet/ethanol: *photon echo*—CH_3CH_2OD host, △ (Ref. 3 and this work), *hole burning*—CH_3CH_2OH host, ■ (Ref. 3 and this work), ◇ [Völker (Ref. 51)], □ [Littau *et al.* (Ref. 5)], CH_3CH_2OD host, + (Ref. 3 and this work); CD_3CD_2OD host, ● (this work).

to an exponential term is found. Fits to just a power law term alone were also found and are listed in Table II. It is clear that the echo temperature dependence cannot be well accounted for by a single power law fit alone, the high temperature dephasing increases more rapidly than T^{α} for α, $1<\alpha<3$. The hole burning data can be fit to a power law temperature dependence; because the activated term is a smaller percentage of the hole burning dephasing, the rollover at high temperature is less noticeable (see Fig. 4). For both echo and hole burning data, however, independent freely varying fits to the two terms in Eq. (24) show very similar activation term values. A consistent, meaningful interpretation of the results can only be achieved by recognizing that hole burning experiments are sensitive to the same fast processes that an echo measures, plus any slower dynamics (spectral diffusion) that are occurring

$$1/T'_{HB} = 1/T'_{PE} + 1/T_{SD}, \tag{25}$$

$$1/T'_{HB} = aT^{\alpha} + b\exp(-\Delta E/kT) + cT^{\beta}. \tag{25a}$$

Here the values of a, α, b, and ΔE are fixed to those fit to photon echo data. The hole burning fit to Eq. (24) combines the a, α, c, β, parameters in a single power law term. By subtracting the echo temperature dependence from the hole burning data, the best fit spectral diffusion parameters c and β are found. These are listed in Table II. Figure 5 plots T_{SD} vs temperature with the best fit power laws and cT^{β} for both resorufin and cresyl violet.

A consistent picture emerges from the temperature signatures of the dephasing times measured by echo and hole burning techniques. At low temperatures, the power law behavior predicted for glass TLS dynamics is observed. These processes occur over both fast and slow time scales and the slower perturbations lead to spectral diffusion yielding the dramatically different values of T'_{HB} relative to T'_{PE}. At higher temperatures, an exponential term due to a fast time scale process gradually takes over. This could be due to the activation of a pseudolocal mode of the chromophore or of the glass molecules themselves. Results on resorufin in fast cooled 94% glycerol/6% water glass show the clearest evidence for an exponentially activated high temperature term.[2,50] Another process that could lead to such a term is activation over a narrow distribution of potential barrier energies.[13] Careful choices of optical probes can distinguish between pseudolocal mode and glass mode activation, as in the rhodamine-B, octadecylrhodamine-B/PMMA study of Elschner *et al.* which showed that the activated process is not a pseudolocal mode.[53]

It is worth considering what leads to the observation of an exponential decay for a photon echo, as is depicted in Fig. 3. If only the nearby environment influenced the dephasing of a chromophore in a glass, it might be expected that the differing local structures would lead to a nonexponential decay response due to a distribution of dephasing rates. Theoretical analysis shows that *dipolar* coupling to TLS, which guarantees that the chromophore will be affected by a large number of nearby and distant perturbers, leads to exponential decays.[22] A further condition for the observation of exponential echo decays is that the distribution of tunneling

TABLE II. Parameters for fits to the photon echo and hole burning data to Eqs. (24) and (25).

Dye/glass	α	a $(\text{ns K}^{\alpha})^{-1}$	b (ns^{-1})	ΔE (cm^{-1})	β	c $(\text{ns K}^{\beta})^{-1}$	χ^2/N[a] (%)
Resorufin/ethanol							
Photon echo	1.3[b]	0.26	230	21			1.4
	2.0[c]	0.16					4.2
Hole burning	1.2[b]	1.7	240	23			0.4
	1.3[c]	1.6					0.7
	1.3[d]	0.26	230	21	1.1	1.5	0.6
Cresyl violet/ethanol							
Photon echo	1.4[b]	0.33	190	15			1.7
	2.0[c]	0.22					5.0
Hole burning	1.2[b]	3.2	280	18			0.6
	1.3[c]	2.9					1.1
	1.4[d]	0.33	190	15	1.1	2.9	0.9

[a] $\chi^2 = \Sigma_j [1 - D_i/F(T_i)]^2$, where D_i are the data points and $F(T_i)$ is the appropriate fit function defined by Eqs. (24) and (25).
[b] Least-squares power law fit to slow T data. This is then subtracted from higher T data, which is then least-squares fit to an exponential term.
[c] Least-squares power law fit only.
[d] Spectral diffusion fit. Hole burning data compared to the echo temperature dependence (fixed) plus an extra power law term cT^{β} (least-squares fit).

rates (R) must be proportional to $1/R$ for a fairly broad range, such that $R_{\min} < 1/T'_{\text{PE}} < R_{\max}$.[2]

It is interesting that at high temperatures in ethanol glass, where dephasing is dominated by the activated process, exponential echo decays are still observed. If the exponential temperature term is due to librational motion of the chromophore (pseudolocal mode), the various sites must have a narrow distribution of frequencies, otherwise a multiexponential decay would result. Another explanation for the exponential high temperature decays is that the activated process is due to a glass mode. Then the chromophores would experience the same averaged perturbation and dephase exponentially. The best fits for ΔE in ethanol Res—$\Delta E = 21$–$22\,\text{cm}^{-1}$, *CV*—$\Delta E = 15$–$18\,\text{cm}^{-1}$, give activation values that are fairly close. Elschner *et al.*[53] also report on the echo temperature dependence of Rhodamine B/ethanol, finding $\Delta E \approx 24\,\text{cm}^{-1}$. If some perturbation of local ethanol frequencies by the differently charged chromophores occurred, an optical phonon mechanism could be responsible for the high temperature term. Dephasing caused by a glass optical phonon was observed in Ref. 53 for ionic dyes in PMMA and also inferred by Furusawa *et al.*[54]

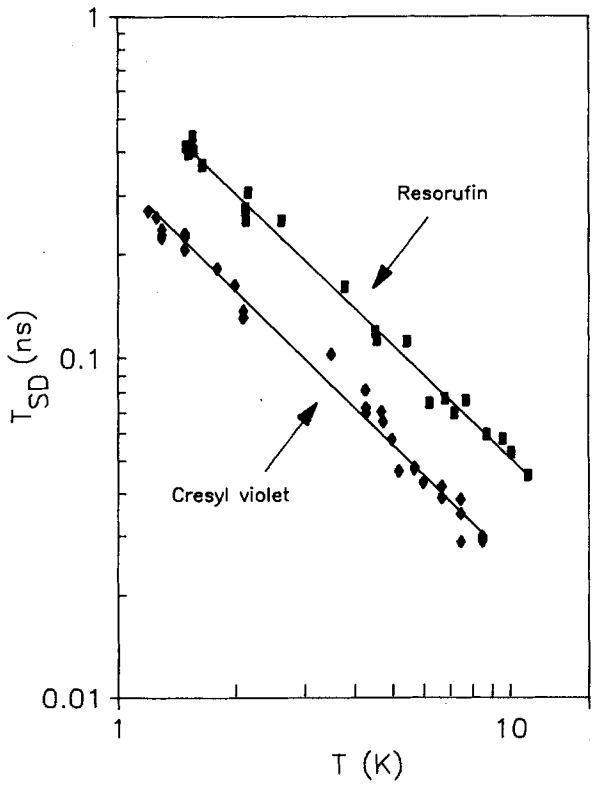

FIG. 5. Temperature dependences of spectral diffusion (T_{SD}) for resorufin/ethanol and cresyl-violet/ethanol. Both sets of data are best fit to a $T^{1.1}$ temperature dependence.

B. Comparison of the different dye's dynamics

Our investigation of a series of dyes in ethanol glass has shown that R_d differs for different chromophores. The average values of R_d at 1.5–1.6 K for the ionic dyes studied are collected in Table III. Three of the dyes exhibit values quite close to the 8.3 calculated from Eq. (21) involving the as-

TABLE III. Dephasing ratios $R_d = T'_{\text{PE}}/T'_{\text{HB}}$ for four ionic dyes in ethanol glass $T = 1.5$–1.6 K. T_w (hole burning) = 200 s.

Dye	Ionic charge	R_d
Resorufin	−1	5.9 ± 0.3
Cresyl violet	+1	8.3 ± 0.3
Sulforhodamine 640	Zwitterion	7.9 ± 0.3
Rhodamine 640	+1	8.5 ± 0.5

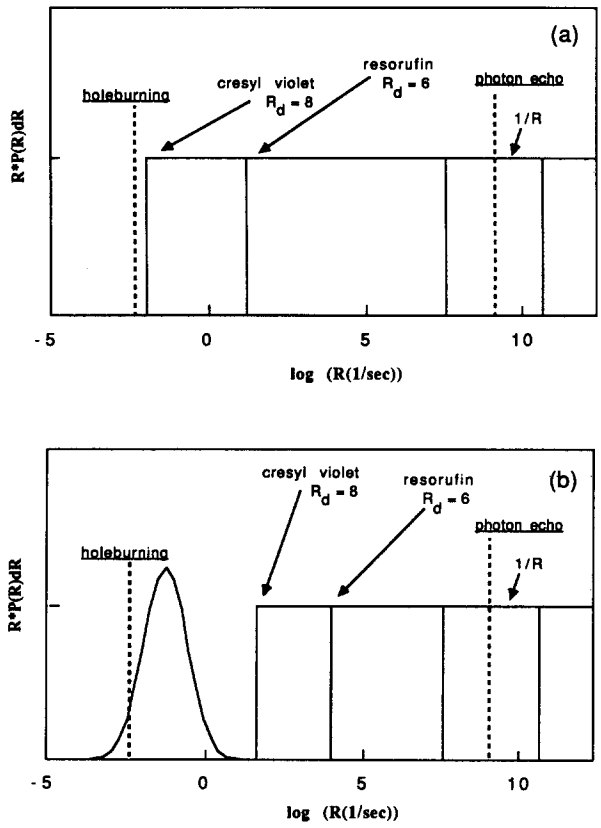

FIG. 6. Two plots of model rate distributions in relation to dephasing results. (a) A $1/R$ rate distribution in comparison with predictions from Eq. (21). The observation of exponential echo decays implies that $P(R) \propto 1/R$ on the echo time scale (vertical bars) for fast rates. Extending this distribution to slower rates implies that resorufin/ethanol would possess a rate cutoff at 1/0.05 s, and cresyl-violet/ethanol would posses a rate cutoff quite close to $1/T_W = 1/200$ s. Hole widths are proportional to the area out to the cut-off rate or $1/T_W$. (b) A qualitative rate distribution based on the recent time-dependent hole burning data of Refs. 4 and 5. A log normal distribution of slow rates is found which is identical to within experimental error for the two dyes resorufin and cresyl violet. Assuming a $1/R$ rate distribution for short times (fast rates), cutoffs at $1/.025$ and $1/1.2\times10^{-4}$ s are calculated from Eq. (21) for the remaining spectral diffusion linewidth.

sumption that the distribution of rates is $P(R) \propto 1/R$. Resorufin, the only anion studied, has a smaller value of R_d. This suggests that the dynamics may have been altered locally by the dye molecules. If the $P(R)$ is still taken as $1/R$, the smaller resorufin value of R_d could result from a cutoff in the rate distribution. Replacing $1/T_W$ by a cut-off rate R_c in Eq. (21) and setting $R_d = 6$, this cutoff can be calculated for resorufin and is $R_c = 22.6\ s^{-1}$. This model is illustrated in Fig. 6(a) for a rate distribution relative to a $\ln(R)$ scale, $P_1(R)d\ln(R) = RP(R)\,dR$. The dye's linewidths (or $1/T'_{HB}$) are proportional to the integral over the distribution of rates, i.e., the area out to their respective cutoffs in Figs. 6(a). The recent time-dependent hold burning work of Littau *et al.*[4,5] have searched for such cutoffs with time-dependent hole burning measurements. They find a more complex rate distribution behavior between $R = 1/100$ ms to $1/6000$ s. In particular, for both resorufin and cresyl violet in CH_3CH_2OH and CD_3CD_2OD, spectral diffusion dependence of the hole width can be well fit by a log normal distribution of relaxation rates[4,5] over this range. Such a distribution might arise from a Gaussian distribution of tunneling parameters λ. Figure 6(b) shows the rate distribution. Since the dyes resorufin and cresyl violet exhibit the same hole broadening behavior at long times,[5] the differences in their dynamic properties must lie in the intermediate time scale, as depicted in Fig. 6(b). In Fig. 6(b), the known short time $P(R) \propto 1/R$ distribution was extended and the difference in dynamics illustrated as a difference in cutoff.

VI. SOLVATION SHELL MODEL CALCULATIONS OF HOLE BURNING LINE SHAPES

The effect of a chromophore-altered local environment on hole burning line shapes can be investigated using the two-domain formalism presented in Sec. IV. What we wish to investigate is the appearance of a hole burning line shape in the presence of altered local dynamic properties. For hole burning line shapes to remain strictly Lorentzian, the spatial integral in Eqs. (9) and (23) must be evaluated with a uniform distribution of TLS parameters over all space. It is interesting to consider what happens to a line shape if a solvation shell effect changes the local environment. An interesting question is "How much could a chromophore alter the local dynamic behavior and still exhibit an apparent Lorentzian hole profile?"

Three regimes, related to the concentration of perturbing glass TLS, the experimental linewidth, the dipolar coupling strength, and the solvation shell radius can be identified in a discussion of solvation shell effects. The first may be termed the inner shell regime. For this situation, all of the perturbations yielding the line shape occur within the solvation shell. The condition for this to hold is $\mathrm{FWHM} \gg D/r_s^3$, perturbations outside the shell radius r_s are negligible in comparison to the linewidth. Invoking the relationship between hole width and $n(T,T_W)$ and D, this implies $n(t,T_W) \gg 1/r_s^3$, must hold. For systems where this is valid, results for different dyes in the same glass will depend on the individual chromophore's effect on the local structure. The only important distribution of rates will be inside the solvation shell and the similarity of this to bulk properties will depend on the details of the solvent–chromophore interaction.

A second set of conditions is the outer shell regime. For a random, low concentration TLS distribution, few perturbers on average will lie near the probe chromophore. The back interaction of a chromophore on the glass will be relatively unimportant in this case, its effects confined to the far wings of the hole profile. The condition for this to hold is $\mathrm{FWHM} \ll D/r_s^3$, and $n(T,T_W) \ll 1/r_s^3$. Perturbations outside the shell radius r_s are the main contributors to the linewidth. No significant solvation shell effect will exist under these conditions.

The third case is the intermediate regime in which TLS existing in the solvation shell and the bulk glass both contribute to the linewidth. When $\mathrm{FWHM} \approx D/r_s^3$ and $n(T,T_W) \approx 1/r_s^3$, this intermediate condition holds. Under these conditions, Eq. (23) may be used to numerically calculate the hole burning line shape and both halves of the equation contribute significantly to the line profile. We proceed to calculate hole burning line shapes by numerically integrating Eq.

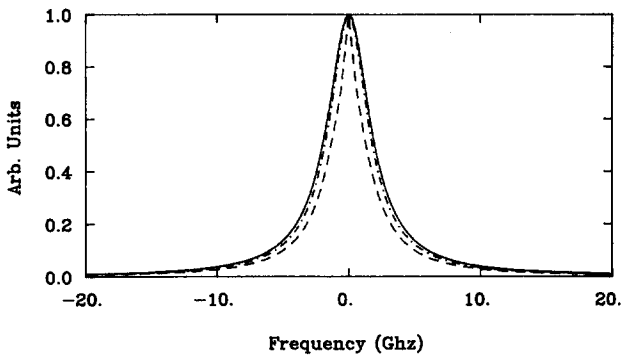

FIG. 7. Hole burning line shapes from the two-domain model inside r_s: —, $r_s = 40$ Å, FWHM = 4.00 GHz; -·-·-, $r_s = 20$ Å, FWHM = 3.63 GHz; and - - -, $r_s = 15$ Å, FWHM = 2.67 GHz. Values for the active TLS concentration $n(T,T_W)$ and the dipolar coupling strength D used throughout are $n_1(T,T_W) = 7\times10^{-4}$ TLS/Å^3, $D = 2.73\times10^{12}$ Hz Å^3.

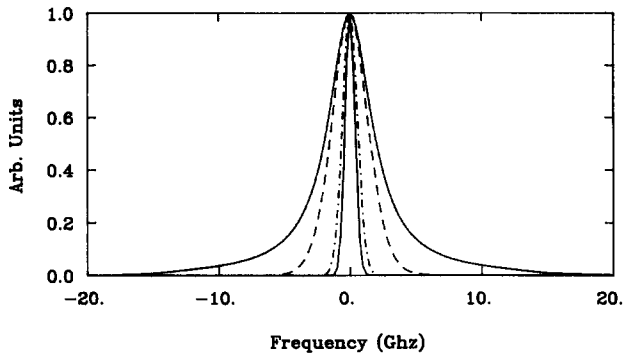

FIG. 8. Hole burning line shapes from the two-domain model outside r_s: (from outer profile in)—, $r_s = 5$ Å, FWHM = 4.00 GHz; - - -, $r_s = 8$ Å, FWHM = 3.13 GHz; -·-·-, $r_s = 15$ Å, FWHM = 1.33 GHz; and —, $r_s = 20$ Å, FWHM = 0.87 GHz. Values for the active TLS concentration $n(T,T_W)$ and the dipolar coupling strength D used throughout are: $n_2(T,T_W) = 7\times10^{-4}$ TLS/Å^3, $D = 2.73\times10^{12}$ Hz Å^3.

(23) and then applying a fast Fourier transform algorithm. Physically plausible values of the active TLS concentration $n(T,T_W) = 7.0\times10^{-4}$ TLS/Å^3 and dipolar coupling strength $D = 2.73\times10^{12}$ Hz Å^3 are used throughout this series of calculations. For uniform spatial distribution of TLS, this would yield a Lorentzian linewidth of 4.00 GHz from Eq. (10). From stark experiments, the change in dipole moment between ground and excited states for ionic dyes is known to be on the order of $\Delta\mu_M = 1$ D.[55] Using the conversion $(1\text{ D})^2 = 1\times10^{36}$ erg cm^3 $= 1.509\times10^{14}$ Hz Å^3, the tunneling system's dipole change would be on the order of $\Delta\mu_{\text{TLS}} = 0.02$ D for the choice of coupling parameter D used.

We first consider the two halves of Eq. (23) separately. This illustrates the limiting behavior of the two-domain model. Figure 7 shows line shapes caused by perturbers inside a spherical shell with radius $r_s = 40$, 20, and 15 Å. For $r_s = 40$ Å, all of the important dynamics are inside the shell radius and the linewidth = 4.00 GHz. Shrinking the size of the spherical region to $r_s = 20$ Å starts to affect the line shape, which narrows to 3.63 GHz. The line profile for $r_s = 15$ Å narrows to 2.67 GHz and is now significantly non-Lorentzian in appearance. Hole burning experiments on dye/solvent systems trapped in porous media might exhibit this type of non-Lorentzian profile. (Note that the unphysical divergence of the line profile at $\Delta\nu = \pm D/r_s$ is avoided in these inner-shell-only calculations by a smooth tapering off of the TLS distribution for $r > r_s$. This is equivalent to a small, diminishing concentration of perturbers external to the r_s cutoff).

Figure 8 shows line profiles calculated for only the outer region $r > r_s$ in Eq. (23). This represents the limit in which *all* of the local dynamics for $r < r_s$ are shut off, as if the local structure is crystallized. For $r_s = 5$ Å, the line shape is indistinguishible from a Lorentzian and has FWHM = 4.00 GHz. This is reassuring, since the dye molecules themselves occupy a volume on this order.[56] As r_s increases, the wings of the line profile, caused by the nearby perturbers, are rapidly lost. The resulting profile is very close to a Gaussian. This is expected from Eq. (23), since for small τ and/or large r_s, the term $\sin^2(D\tau x) \approx (D\tau x)^2$. This leads to a Gaussian decay of the correlation function (see Fig. 2) and therefore a Gaussian line profile in this limit (Ref. 31 has a similar discussion for spin-resonance processes).

We now calculate the hole burning line profiles for the combined solvation shell + bulk dynamics (inner shell plus outer shell). The effect of altering the local dynamics is investigated by lowering the value of $n(T,T_W)$ inside the solvation shell. Such a reduction might occur if an ordering of the local solvent dipolar molecules around an ionic chromophore lead to a lower concentration of TLS. It is known from hole burning experiments on resorufin in ethanol[49,50] that, after a bulk transition from the amorphous phase to the plastic crystalline phase, the dynamics are reduced by a factor of 10, most likely due to a reduction in $n(T,T_W)$. The plastic crystalline phase is orientationally disordered, but translationally it is somewhat ordered. A postulated back reaction of the chromophore on the solvent might induce some similar ordering locally. Another way in which a reduction in local dynamics could occur would be if the chromophore, through bonding or electrostatic effects, increased TLS potential barriers, slowing some of the tunneling processes out of the experimental time scale. Figure 9 shows schematic distributions of rates illustrating these two cases. In Fig. 9(a), the distribution of rates in the shell and the bulk have the same functional form, but the magnitude of the concentration is reduced by 25% locally. Figure 9(b) shows an inner shell rate distribution in which a 25% subset of the dynamic processes have been slowed down and are now beyond the experimental time scale.

Figure 10 plots line profiles for $n_1(T,T_W) = Cn_2(T,T_W)$, where C varies from 1.0 to 0.25. As the active TLS concentration in the inner region is changed from 100% to 25% of the bulk value, the line narrows from 4.00 to 1.79 GHz, a significant change. The four model hole shapes in Fig. 10 show the progression from no solvation shell effect, to a situation in which 75% of the local dynamics have been lost. The solvent shell altered curves in Fig. 10 are compared to Lorentzians in Fig. 11. The solid curves in curves in Fig. 11 are Lorentzians with the same height and FWHM as the three shell calculations plotted with the dashed curves.

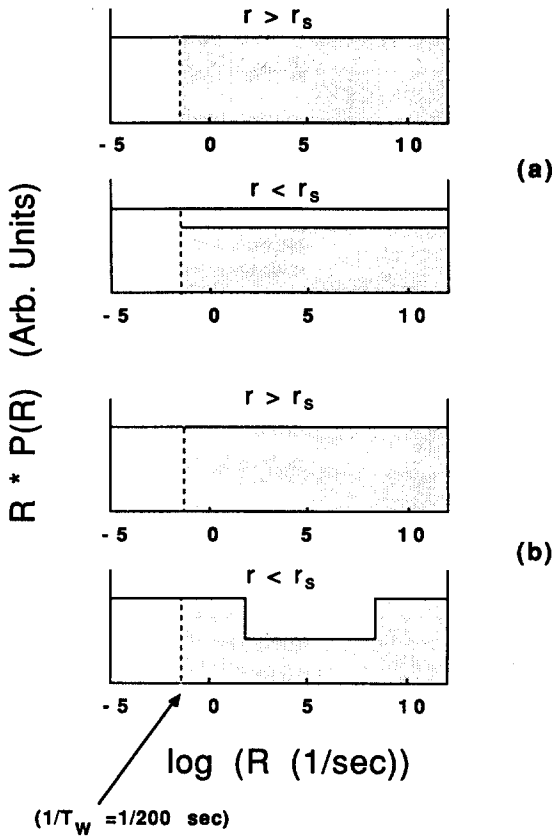

FIG. 9. Schematic rate distribution functions $P(R)$ vs log (R). (a) The concentration of TLS varies inside and outside the shell radius r_s. (b) A subset of the rates inside the solvation shell have been slowed to beyond the experimental time scale.

As Fig. 11 illustrates the line profiles remains close to Lorentzians. Only very large perturbations of the local dynamics will give rise to a hole shape that is distinguishible from a Lorentzian. Given typical signal-to-noise ratios in hole

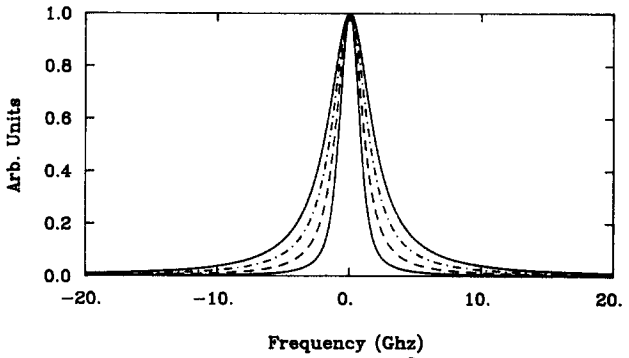

FIG. 10. Line shapes obtained from the two domain theory in which the concentration of TLS is reduced in the solvent shell (1) relative to the bulk (2). Composite line shape for $r_s = 15$ Å for: (from outer profile in)—, $n_1(T,T_W) = n_2(T,T_W)$, FWHM = 4.00 GHz; -·-·, $n_1(T,T_W) = 0.75\, n_2(T,T_W)$, FWHM = 3.15 GHz; - - -, $n_1(T,T_W) = 0.50 n_2\ (T,T_W)$, FWHM = 2.40 GHz; —, $n_1(T,T_W) = 0.25\ n_2(T,T_W)$, FWHM = 1.79 GHz. Values for the active TLS concentration $n(T,T_W)$ and the dipolar coupling strength D used throughout are $n(T,T_W) = 7\times10^{-4}$ TLS/Å^3, $D = 2.73\times10^{12}$ Hz Å^3. The widest curve is a true Lorentzian. The inner three curves are not true Lorentzians. The small deviation from Lorentzian shapes is shown in Fig. 11.

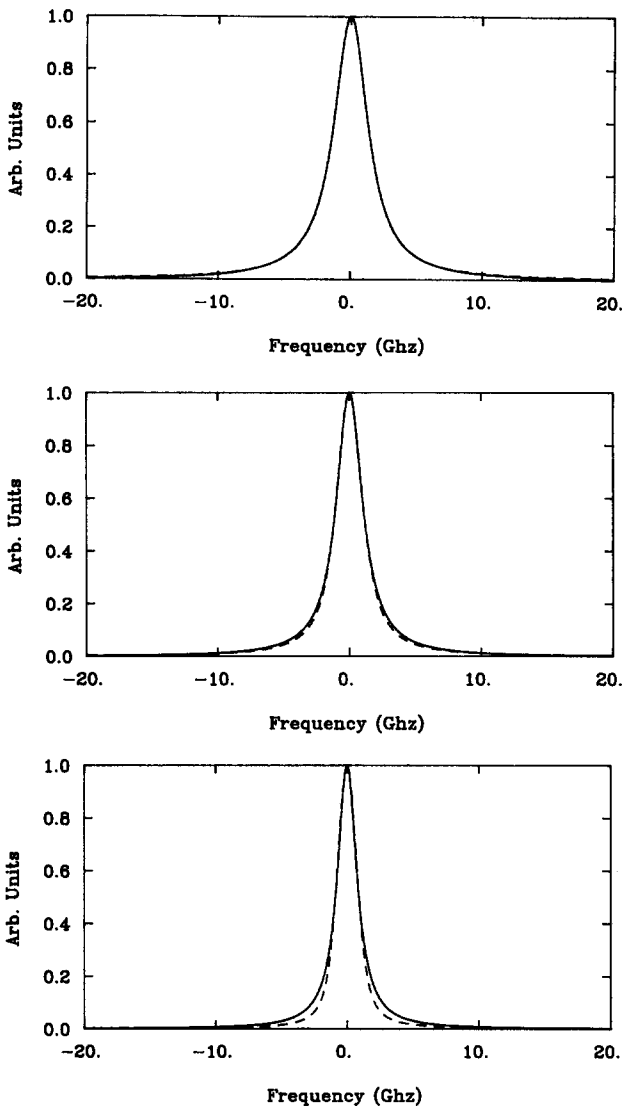

FIG. 11. Line shapes obtained from the two domain theory in which the concentration of TLS is reduced in the solvent shell (1) relative to the bulk (2). (a) $n_1(T,T_W) = 0.75 n_2\ (T,T_W)$; (b) $n_1(T,T_W) = 0.50 n_2(T,T_W)$; (c) $n_1(T,T_W) = 0.25 n_2(T,T_W)$. The solid lines are true Lorentzians with the same height and FWHM. The two-domain theory line profiles differ very little from a Lorentzian shape even when local dynamics have been perturbed by more than 50%.

burning experiments, even the curve in Fig. 11(c) could easily be taken to be a Lorentzian. Therefore, the observation of an apparent experimental Lorentzian hole shape cannot be used to rule out solvent shell effects. We conclude that significant alteration of local glass dynamics could occur without the effect manifesting itself in measurements taken on a single time scale on a single dye molecule.

A change on the order of 30% in the local dynamics is necessary to cause the variation of R_d values observed between resorufin and the other dyes investigated. Resorufin is the only anionic dye that has been studied so far. To learn if there is a systematic dependence on chromophore charge, measurements on other anions would be useful. Mapping out more of the distribution of rates with a combination of experimental techniques should provide further insight into solute ion-dependent properties in ethanol glasses and on what time scale solute–solvent effects are manifested.

VII. CONCLUDING REMARKS

This paper has presented experimental and theoretical results on optical probes of low temperature dynamics in glasses. The dynamic times measured by both the two-pulse photon echo and optical hole burning techniques are both well fit by functions of the general form $1/T_{\rm exp} = aT^{\alpha} + b\exp(-\Delta E/kT)$. The power law characteristic of glass TLS dynamics is predominant for $T < 4$ K. With rising temperatures, the exponential term, with ΔE values ranging from 15–23 cm^{-1}, gradually takes over. The lack of an observed deuteration effect on photon echo[2] and hole burning[2,3] measurements on ionic dyes in CH_3CH_2OH and CH_3CH_2OD, and CD_3CD_2OD, implies that hydrogen tunneling is not the perturbing TLS processes at the temperatures and time scales studied. Hole burning linewidths of ionic dyes in ethanol glass are dominated by spectral diffusion.

The comparison with photon echo results shows that $R_d = T'_{\rm PE}/T'_{\rm HB}$ has values ranging from six to nine. Different dyes in the same glass show differing values of R_d. In particular, the only anion studied, resorufin ($R_d = 5.9$), differs from the three other dyes, for which $R_d = 8$–9. If only dynamics of the bulk glass were responsible for the perturbation of the chromophores, theoretical analysis shows that R_d would have a constant value independent of the dye molecule. Different dye molecules, particularly positive vs negative ions, will have different solvent shell structures. These differing structures will be frozen in when the glass is formed. Differences in solvent shell structures can give rise to distinct local dynamics, leading to dye-dependent optical dephasing. A simple two-domain model for solvation is investigated, in which glass dynamics in a solvent shell are different from the bulk. Model line shape calculations show that differences between local and bulk dynamics can cause large changes in measured linewidths, while leaving hole profiles essentially indistinguishible from Lorentzian shapes. Therefore, comparing the ratio of hole burning to echo linewidth R_d for different chromophores in the same glass can be used as a probe of solvent shell dynamics as well as bulk dynamics.

ACKNOWLEDGMENTS

This work was supported by the National Science Foundation Division of Material Research (DMR 87-18959). Computations were performed using equipment provided by the National Science Foundation Computing Grant (CHE 88-21737). Y. S. Bai and K. Littau are thanked for sharing their insights on glass dynamics. A. Stein is thanked for his help with the measurement of emission lifetimes with equipment courtesy of the Stanford Center for Materials Research. L. R. N. thanks the Fannie and John Hertz Foundation for a Graduate Fellowship.

[1] C. A. Walsh, M. Berg, L. R. Narasimhan, and M. D. Fayer, J. Chem. Phys. **86**, 77 (1987).
[2] M. Berg, C. A. Walsh, L. R. Narasimhan, K. A. Littau, and M. D. Fayer, J. Chem. Phys. **88**, 1564 (1988).
[3] L. R. Narasimhan, D. W. Pack, and M. D. Fayer, Chem. Phys. Lett. **152**, 287 (1988).
[4] K. Littau, Y. S. Bai, and M. D. Fayer, Chem. Phys. Lett. **159**, 1 (1989).
[5] K. Littau, Y. S. Bai, and M. D. Fayer, J. Chem. Phys. (accepted).
[6] L. R. Narasimhan, K. A. Littau, D. W. Pack, Y. S. Bai, A. Elschner, and M. D. Fayer, Chem. Rev. (in press).
[7] R. M. MacFarlane and R. M. Shelby, in *Laser Spectroscopy IV*, edited by H. P. Weber and W. Lüthy (Springer, Berlin, 1983), p. 113.; R. M. Shelby and R. M. MacFarlane, J. Lumin. **31&32**, 839 (1984).
[8] K. K. Rebane, Cryst. Lattice Def. Amorph. Mater. **12**, 427 (1985).
[9] K. K. Rebane and A. A. Gorokhovskii, J. Lumin. **36**, 237 (1987).
[10] H. Fidder, S. de Boer, and D. A. Wiersma, Chem. Phys. **139**, 317 (1989).
[11] A. Rebane and D. Haarer, Opts. Commun. **70**, 478 (1989).
[12] W. Breinl, J. Friedrich, and D. Haarer, Phys. Rev. B **34**, 7271 (1986).
[13] W. Köhler, J. Zollfrank, and J. Friedrich, Phys. Rev. B **39**, 5414 (1989).
[14] Y. S. Bai and M. D. Fayer, Chem. Phys. **128**, 135 (1988).
[15] Y. S. Bai and M. D. Fayer, Phys. Rev. B **37**, 10440 (1988).
[16] Y. S. Bai and M. D. Fayer, Comments Cond. Mater. Phys. **14**, 343 (1989).
[17] Y. S. Bai and M. D. Fayer, Phys. Rev. B **39**, 11066 (1989).
[18] D. L. Huber, J. Lumin. **36**, 307 (1987).
[19] W. O. Putikka and D. L. Huber, Phys. Rev. B **36**, 3436 (1987).
[20] M. J. Weber, J. Lumin. **36**, 179 (1987).
[21] *Optical Spectroscopy of Glasses*, edited by I. Zschökke (Reidel, Dordrecht, 1986).
[22] D. L. Huber, M. M. Broer, and B. Golding, Phys. Rev. Lett. **52**, 2281 (1984).
[23] O. Haida, H. Suga, and S. Seki, J. Chem. Thermodyn. **9**, 1133 (1977).
[24] P.-G. Jönsson, Acta Crystallog. Sect. B **32**, 232 (1976).
[25] R. W. Olson, H. W. H. Lee, F. G. Patterson, and M. D. Fayer, J. Chem. Phys. **76**, 31 (1982).
[26] H. Tanaka, F. Kokai, J. Brauman, and M. D. Fayer, Chem. Phys. Lett. **142**, 371 (1987).
[27] F. Kokai, H. Tanaka, J. Brauman, and M. D. Fayer, Chem. Phys. Lett. **143**, 1 (1988).
[28] D. W. Pack and M. D. Fayer, Chem. Phys. Lett. (accepted).
[29] P. Hu and S. R. Hartmann, Phys. Rev. B **9**, 1 (1974).
[30] P. Hu and L. R. Walker, Phys. Rev. B **18**, 1300 (1978).
[31] J. R. Klauder and P. W. Anderson, Phys. Rev. **125**, 912 (1962).
[32] W. B. Mims, Phys. Rev. **168**, 37 (1968).
[33] *Amorphous Solids: Low-Temperature Properties*, edited by W. A. Phillips (Springer, Berlin, 1981).
[34] A. M. Stoneham, Rev. Mod. Phys. **41**, 82 (1969).
[35] J. Baumann and M. D. Fayer, J. Chem. Phys. **85**, 4087 (1986).
[36] J. L. Black and B. I. Halperin, Phys. Rev. B **16**, 2879 (1977).
[37] A. Abragam, *The Principles of Nuclear Magnetism* (Clarendon, Oxford, 1961) Chap. IV, Sec. IV B.
[38] W. J. C. Grant and M. W. P. Strandberg, Phys. Rev. A **135**, 715 (1964); **135**, 727 (1964); W. J. C. Grant, Ph.D. thesis, Department of Physics, MIT, Cambridge, Mass. 1962 (unpublished).
[39] T. L. Reinecke, Solid State Commun. **32**, 1103 (1979).
[40] P. W. Anderson, B. I. Halperin, and C. M. Varma, Philos. Mag. **25**, 1 (1972).
[41] W. A. Phillips, J. Low Temp. Phys. **7**, 351 (1972).
[42] R. C. Zeller and R. O. Pohl, Phys. Rev. B **4**, 2029 (1971).
[43] J. Jäckle, Z. Phys. **257**, 212 (1972).
[44] R. Jankowiak, G. J. Small, and K. B. Athreya, J. Phys. Chem. **90**, 3896 (1986); R. Jankowiak, G. J. Small, and B. Ries, Chem. Phys. **118**, 223 (1987).
[45] R. Maynard, R. Rammal, and R. Suchail, J. Phys. Lett. **41**, L291 (1980).
[46] R. Maynard, R. Rammal, and R. Suchail, J. Phys. Lett. **41**, L614 (1980).
[47] C. A. Walsh, M. Berg, L. R. Narasimhan, and M. D. Fayer, Acc. Chem. Res. **20**, 120 (1987).
[48] M. D. Levenson, *Introduction to Nonlinear Laser Spectroscopy* (Academic, New York, 1982).
[49] R. Van Den Berg and S. Völker, Chem. Phys. Lett. **137**, 201 (1987).
[50] C. A. Walsh, M. Berg, L. R. Narasimhan, and M. D. Fayer, Chem. Phys. Lett. **139**, 485 (1987).
[51] S. Völker, J. Lumin. **36**, 251 (1987).
[52] B. Jackson and R. Silbey, Chem. Phys. Lett. **99**, 331 (1983).
[53] A. Elschner, L. R. Narasimhan, and M. D. Fayer, Chem. Phys. Lett. (to be submitted).
[54] A. Furusawa, K. Horie, and I. Mita, Chem. Phys. Lett. **161**, 227 (1989).
[55] A. Renn, S. E. Bucher, A. J. Meixner, E. C. Meister, and U. P. Wild, J. Lumin. **39**, 181 (1988).
[56] R. S. Moog, M. D. Ediger, S. G. Boxer, and M. D. Fayer, J. Phys. Chem. **86**, 4694 (1982).